NANO LETTERS

pubs.acs.org/NanoLett

Extensively Chaotic Motion in Electrostatically Driven Nanowires and Applications

Qingfei Chen,*,† Liang Huang,† Ying-Cheng Lai,†,‡,§ Celso Grebogi,§ and David Dietz||

†School of Electrical, Computer, and Energy Engineering, Arizona State University, Tempe, Arizona 85287, ‡Department of Physics, Arizona State University, Tempe, Arizona 85287, §Institute for Complex Systems and Mathematical Biology, King's College, University of Aberdeen, Aberdeen AB24 3UE, U.K., and ||Air Force Research Laboratory, AFRL/RDHE, 3550 Aberdeen Avenue SE, Kirtland AFB, New Mexico 87117

ABSTRACT We carry out a detailed bifurcation analysis for a common class of electrostatically driven nanowires in a multiphysics model. A finding is that the nanoscale system can exhibit distinct chaotic states: chaos with symmetry breaking and extensive chaos possessing the full symmetry of the system. Potential applications such as nanoscale random number generator and controlling extensive chaos to achieve desirable performance are articulated.

KEYWORDS Nanowire, nonlinear dynamics, extensive chaos, crisis, random number generator

Nanoelectromechancal (NEM) systems are characterized by their small size, extremely low power consumption, and ultrafast speed. Due to these benefits, the fundamentals of NEM systems have been investigated and they have also been explored widely for applications ranging from zeptogram scale mass sensing[1] to single electron spin detection[2] and RF communication.[3] In the nonlinear regime of NEM systems, complex phenomena such as spring harding,[4] hysteresis,[5] and pull-in phenomena[6] have been investigated experimentally. Parallel to this, there have been theoretical and computational studies on the critical pull-in voltage value,[7] dynamical range,[8] excitation of nonplanar motion,[9] boundaries of basins of attraction,[5] etc. The nonlinear dynamical properties of NEM systems can be exploited for applications. For example, suspended carbon nanotubes can be used as memory devices based on their nonlinear pull-in behavior,[10] nanotube-based tweezers[11] are actuated by nonlinear electrostatic force, and nonlinear NEM resonators can be used to improve the measurement precision of resonant frequency[12] and mass detection sensitivity.[13]

The intrinsic nonlinear dynamical characteristics of NEM systems lead naturally to the question as to whether chaos can arise and, more importantly, whether one can explore chaos to enhance its applicability. For the class of systems of larger scale known as microelectromechanical (MEM) systems, chaos can occur and has been examined. For example, chaotic oscillations have been found in the cantilever of atomic force microscopy,[14] in the electrostatic tuning comb drive actuator for signal encryption,[15] and in nonlinear, parametrically excited resonators.[16] In electrostatically driven MEM systems, the period-doubling route to chaos has been found.[17,18] Despite the occurrence of chaos in MEM systems, there has been little work on chaos in NEM systems.[19] Especially for suspended nanowire resonators it has been assumed in most previous works that the oscillation occurs in a single plane. Only recently, Conley et al.[9] obtained analytically and numerically the onset of nonplanar motion. The onset value agrees well with published experimental results, leading to their conjecture that exploiting nonplanar and other nonlinear dynamical phenomena in such resonators can find applications in signal processing, filtering and encryption. Due to the potential advantages offered by chaos in dynamical systems[20] and due to the vast potential of nanoscale devices, we investigate their dynamics using a partial differential equation (PDE) model[9] and its consequences with an eye toward applications.

In this Letter, we present the first evidence of extensive chaos in NEM systems. The class of nanoscale systems that we explore is electrostatically driven Si nanowires,[21,22] which is theoretically modeled and discussed in the work of ref 9. By design, a nanowire is supposed to oscillate in a plane. However, nonplanar motion of the wire can occur under certain conditions.[9] We find that, in the regime of nonplanar motion, chaos can be rather common. In addition, the dynamical phenomenon of crisis can occur where two symmetry-broken chaotic attractors can collide simultaneously with their basin boundaries to form a much larger, single chaotic attractor possessing the full symmetry of the system. Chaotic oscillations associated with the resulting attractor are extensive in the sense that they occur in phase-space regions even at all scales that were inaccessible before the crisis. We conduct a bifurcation analysis to uncover the

* To whom correspondence should be addressed. E-mail: qchen20@asu.edu.
Received for review: 08/25/2009
Published on Web: 01/07/2010

DOI: 10.1021/nl902775m | *Nano Lett.* **2010,** *10,* 406-413

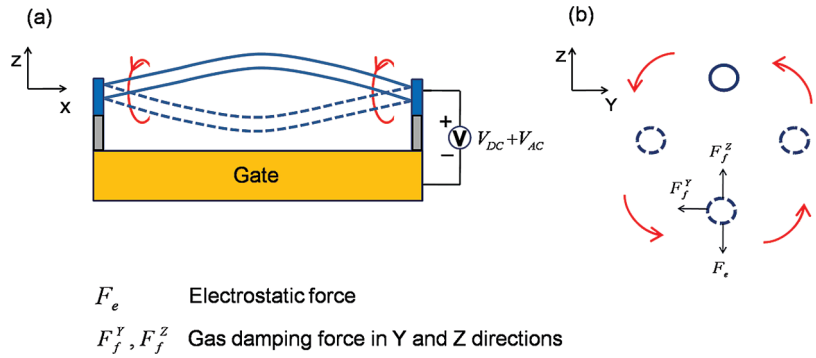

FIGURE 1. (a) An electrostatically driven, suspended nanowire and (b) illustration of wire's rotation associated with nonplanar motion.

dynamical and physical mechanism leading to extensive chaos and articulate potential applications. We mention that our work is inspired by ref 9, where the prediction of nonplanar motion makes possible generating extensive chaos in nanowire systems.

Figure 1a shows the device configuration of a suspended nanowire.[9] It is a solid structure with two ends bridging the sidewalls. The electrostatically driving force is exerted from the gate electrode. Under a small force, the nanowire oscillates vertically in the Z direction as a doubly clamped beam. However, when the applied voltage is sufficiently large to yield substantial bending and consequently strong axial stress, the vertical vibration (planar vibration) is no longer stable and the wire tends to bend to its sides (Y direction) and rotate in the $Y-Z$ plane. A schematic illustration of this rotating motion is shown in Figure 1b.

A dynamical analysis of electrostatically driven nanowires requires combined solutions to the mechanical, electrical, and fluid equations governing the physics and the motion of the wire. In the following we treat these respective aspects.

Mechanical Equations. Here we consider a partial differential equation (PDE) model to study the chaotic whirling motions of suspended nanowires. The formula of the nanowire mechanical PDE equation together with electrostatic force model are previously proposed and studied in ref 9, where the theoretical and simulation results from this model have been compared with several experimental results, with good agreement. Consider the circular cross-sectional area A (radius r), the PDEs governing the displacements $Y(x, t)$ and $Z(x, t)$ of the wire in the Y and Z directions, respectively, are

$$\rho A Z_{tt} + EIZ_{xxxx} - \frac{EA}{2L} Z_{xx} \int_0^L (Y_x^{\,2} + Z_x^{\,2})\, dx = F_f^Z + F_e \tag{1}$$

$$\rho A Y_{tt} + EIY_{xxxx} - \frac{EA}{2L} Y_{xx} \int_0^L (Y_x^{\,2} + Z_x^{\,2})\, dx = F_f^Y$$

where F_e is the electrostatic force on the wire, F_f^Y and F_f^Z are the viscous damping force in the Y and Z directions, respectively, E is Young's modulus, and $I = \pi r^4/4$ is the moment of inertia of the wire's cross-sectional area. Here we briefly show the derivation of electrostatic force model which is skipped in literature.[9] The electrostatic force on a bending nanowire depends on its deflection shape and is spatially dependent. A nanowire actuated by electrostatic force can be approximated by a sequence of short-length wire segments, each segment being parallel to the planar gate electrode. The segment at position x, in conjunction with the gate electrode, then forms a capacitor charged by the driving voltage with capacitance per unit length given by $C(x, t) = 2\pi\varepsilon\, dx/\{\ln[4(g_0 + u(x))/d]\}$, where g_0 is the (x-independent) wire-center-to-electrode gap when the entire wire is in the inactivated state, $u(x, t)$ is the instantaneous deviation of the segment's Z-coordinate from g_0 [so $g_0 + u(x, t) = Z(x, t)$], d is the wire diameter, and ε is the dielectric constant of the homogeneous gaseous medium in which the NEM is immersed. It is assumed that, for all t, $d \ll g_0 + u(x, t)$ so that the expression for $C(x, t)$ is valid. For a single segment at position x, the work of electrostatic force of pulling the nanowire with distance of $u(x)$ toward the gate electrode from original position is

$$W(x, t) = \frac{C(x, t)V^2}{2} - \frac{C_0(x, t)V^2}{2} = \frac{\pi\varepsilon V^2\, dx}{\ln\{4[g_0 + u(x)]/d\}} - \frac{\pi\varepsilon V^2\, dx}{\ln\{4g_0/d\}}$$

where $V(t) = V_{DC} + V_{AC}\cos(2\pi ft)$ is the combination of a dc bias voltage and an ac voltage of frequency f. The electrostatic force per unit length acting at x on the nanowire at time t is then

$$F_e(x) = \frac{dW(x)}{du}\frac{1}{dx} = \frac{-\pi\varepsilon V^2}{(g_0 + u(x))\{\ln[4(g_0 + u(x))/d]\}^2} \tag{2}$$

Gas Damping Force. To achieve high sensitivity or large dynamical response of NEMS sensors and actuators which utilize their resonant behavior,[23,24] many fundamental studies on NEMS resonators were performed in ultrahigh vacuum and at low temperatures to reduce the damping effect. The

DOI: 10.1021/nl902775m | *Nano Lett.* **2010,** *10,* 406-413

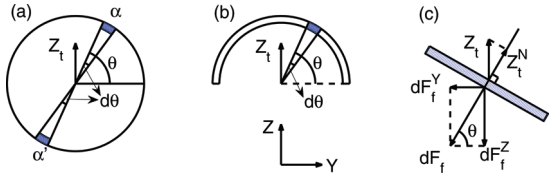

FIGURE 2. (a) Cross-sectional view of a nanowire moving in the *Z* direction, (b) equivalent shell structure subject to the same damping force, and (c) small section of shell of angular extension dθ.

resulted damping coefficient can thus be decreased by hundreds of times,[25] resulting in very weak dissipation in the system which is beneficial for NEMS devices that utilize their resonant behaviors. However, in forced vibrating string or beam systems, it is known that to generate and utilize chaotic motions, certain amount of damping is necessary.[26] Otherwise, the complex motions would be easily eliminated by the crisis mechanism.[27] Another concern of ultrahigh vacuum and low temperature is that these rigid working conditions impose difficulties in the packaging and integration of NEMS devices, which could hamper the potential range of applications. On the other hand, several recent experimental works[28−30] show that actuation and sensing of NEMS vibration under room conditions (300 K temperature and 1 atm pressure) can be successfully achieved. In this paper we thus study devices operated under room environment, which is the easiest accessible condition. Due to the small scale of the wire size, under room conditions, its vibrations in a gaseous medium (e.g., air) are governed by molecular regime physics for which the drag force on the wire is due to momentum exchange with the surrounding gas molecules. Here, we derive the drag force on the wire along the *Z* direction (the force in the *Y* direction has the same form). Consider the cross-sectional view of the nanowire moving in the *Z* direction, as shown in Figure 2a. We divide the cross section into a set of segments, each with small angle increment dθ. Examining the two symmetrically opposite segments shown in Figure 2a, we see that the frictional force due to air on each segment is the same as that on one of the thin camber shells, as shown in Figure 2b. Thus, in the molecular regime, the structure shown in Figure 2a is subject to the same damping force as the one in Figure 2b. To obtain the full damping force on the structure in Figure 2b, we first consider a small segment at angle θ, as shown in Figure 2c. This small segment of angular extension dθ can be regarded as a thin rectangular plate in a $Y-Z$ plane tilted by angle ($\pi/2 - \theta$), moving in the Z direction with velocity Z_t. Since Z_t can be decomposed into a component moving in the direction normal to the surface (Z_t^N) and another component parallel to the surface that does not contribute to the frictional force on the thin plate, only Z_t^N contributes to the drag. The drag force on a thin plate moving in a gas in the direction normal to its surface at speed Z_t^N is given by

$$F_f^N = \frac{PA_s}{v_T} Z_t^N \tag{3}$$

where P is the pressure of the gas, A_s is the plate surface area, $v_T = (K_B T/m)^{1/2}$ is the molecule velocity at temperature T, m is the molecule mass, and K_B is Boltzmann constant. Force per unit x direction length opposing the motion of this small segment can then be written as

$$dF_f^Z = dF_f \sin(\theta) = \frac{Pr \sin^2(\theta)}{v_T} d\theta\, Z_t \tag{4}$$

The total drag force acting on the camber shell per unit length, which is equal to that acting on the nanowire per unit length, is

$$F_f^Z(x,t) = \int_0^\pi \frac{Pr \sin^2(\theta)}{v_T} d\theta\, Z_t(x,t) = \frac{\pi P d}{4 v_T} Z_t(x,t) \tag{5}$$

for the wire segment located at x. Similarly, we have

$$F_f^Y(x,t) = \frac{\pi P d}{4 v_T} Y_t(x,t) \tag{6}$$

One can see that the damping coefficient of the round nanowire compared to the square one with the same width only drops by a factor of $\pi/4$. We have examined the theoretical gas-damping model with several experimental data for different sizes of nanowires working under room conditions.[30] The theoretical results of quality factors obtained by the gas-damping model agree reasonably with the experimental data to within about 20 % on average.

Multiphysics simulation of the nanowire is carried out based on eqs 1, 2, 5, and 6. In our simulation, a standard finite element method (FEM)[31] is employed to deal with the spatial differential and integral terms in the equation and a forward fourth-order Runge−Kutta method is employed to perform the time integration. The method is validated by using an electrostatic MEMS fixed−fixed beam model including nonlinear elastic term and compaired with the results generated by a different numerical method.[32] In our simulations, we use a 3 μm × 20 nm ($L \times d$) doubly clamped nanowire made of silicon. The gate trench height is $h = 0.2$ μm. The device is operated under room conditions ($P = 1$ atm and $T = 300$ K). The natural frequency of device is obtained as $f_0 = 3.56(EI/(L^4 \rho A))^{1/2}$.[9] Here, we set the frequency of the ac voltage to be $f = 3f_0$. For silicon, the material parameters are $E = 169G$Pa and $\rho = 2332$ kg/m^3.

DOI: 10.1021/nl902775m | *Nano Lett.* **2010,** *10,* 406-413

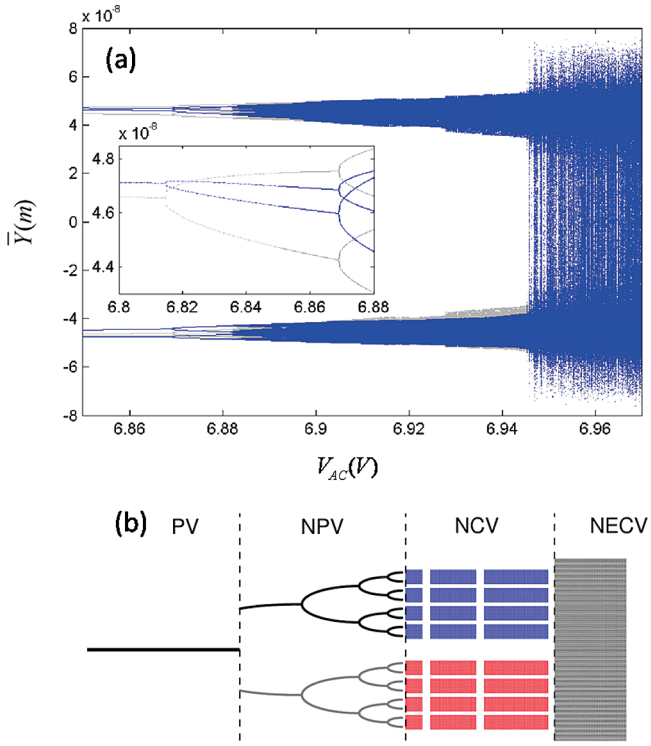

FIGURE 3. (a) A typical bifurcation diagram for the nanowire: local extrema of $Y(L/2)$ versus V_{AC}. The detail of a part of the period-doubling bifurcation is shown in the inset. (b) Schematic illustration of the occurrence of distinct oscillatory states.

The molecular mass of air is $m = 5.6 \times 10^{-26}$ kg. Thirteen spatial elements and time step of (2×10^{-3})Pe, where Pe $= 1/f_0$ is the period of the resonant state, are used to solve the nonlinear PDE.

Our calculations have revealed the existence of four characteristically different vibration states of the nanowire as the ac voltage is increased. A representative bifurcation diagram is shown in Figure 3a, where the possible local extrema in the displacement of the center of the nanowire in the Y direction are plotted as a function of the ac voltage. A schematic diagram of the bifurcation process is shown in Figure 3b. In the simulation, the dc bias voltage is set to be $V_{DC} = 12$ V. As V_{AC} is increased from zero, the system first reaches a planar vibration state, denoted as PV, where the motion of the device is time periodic and is confined physically in the $X-Z$ plane. In this case, the displacement and the velocity of the nanowire in the Y direction are zero, corresponding to a single point at the origin of the two-dimensional phase-space slice defined by $[\bar{Y} \equiv Y(x = L/2), d\bar{Y}/dt]$, shown as a cross in Figure 4a. As V_{AC} is increased through a critical value $V_{AC}^{(1)} \approx 0.5947$ V, the planar motion becomes unstable and the nanowire begins to exhibit non-planar vibrations and rotations in the phase space, as shown in Figure 4b. We denote this state as NPV. As V_{AC} is increased further, a cascade of period-doubling bifurcations occurs, which leads to chaotic vibrations for $V_{AC} > V_{AC}^{(2)} \approx 6.8818$ V. In this regime, there is symmetry breaking in the sense that for any initial condition the trajectory lands on a chaotic attractor that does not possess the full symmetry of the system. In fact, there exist two symmetric attractors, each with its own basin of attraction, as shown in Figure 4c. We denote such a chaotic state as NCV (nonplanar chaotic vibration). Finally, as V_{AC} is increased through another critical point $V_{AC}^{(3)} \approx 6.9457$ V, the two symmetrical attractors merge to form an extensive chaotic attractor, as shown in Figure 4d. In this state, the system symmetry $Y(-x) = -Y(x)$ is restored, and the gaps present in each symmetry-broken chaotic attractor in the NCV regime and the gap between the two symmetrical attractors are filled.

For a nanowire under large electrostatic force, the transition between the PV and the NPV state can be understood physically, as follows. In a PV state, the vibration amplitude of the nanowire in the Z direction is relatively small but it increases as the external ac voltage is increased. For $V_{AC} = V_{AC}^{(1)}$, the stress induced by the vibration of the wire in the axial direction reaches a critical value that can barely keep the motion of the wire in the $X-Z$ plane. As $V_{AC}^{(1)}$ is exceeded, the stress is no longer able to keep the wire in this plane. To gain more insight into the transition, we examine the equation of motion in the Y direction:

$$\rho A Y_{tt} + EIY_{xxxx} - \frac{\pi Pd}{4v_T} Y_t - \frac{EA}{2L} Y_{xx} \int_0^L (Y_x^2 + Z_x^2)\, dx = F_f^Y$$

This is basically the equation of motion for a parametric resonator driven by the term $\int_0^L Z_x^2\, dx$. To investigate the stability of the planar vibration $\mathbf{N} \doteq \{Z(x,t), \dot{Z}(x,t), Y(x,t), \dot{Y}(x,t) | Y(x,t) = 0, \dot{Y}(x,t) = 0\}$, we focus on the perturbed dynamical equations near $\mathbf{N}$

$$\rho A Z_{tt} - \frac{\pi Pd}{4v_T} Z_t + EIZ_{xxxx} - \frac{EA}{2L} Z_{xx} \int_0^L Z_x^2\, dx = F_e$$

$$\rho A \delta Y_{tt} - \frac{\pi Pd}{4v_T} \delta Y_t + EI \delta Y_{xxxx} - \frac{EA}{2L} \delta Y_{xx} \int_0^L Z_x^2\, dx = 0$$

The behavior of the perturbed vibration can be characterized by the escape exponent defined by $M = \lim_{t\to\infty} \ln[(\delta(x,t))/(\delta(0,x))]/t$ for any $0 < x < L$. If $\mathbf{N}$ is stable, we have $\delta(t,x) \to 0$ as $t \to \infty$ so that $M < 0$. If $\mathbf{N}$ is unstable, we have $\delta(t,x) \to \infty$ as $t \to \infty$ and so M becomes positive. Near the transition between PV and NPV states, we expect to see a rather abrupt change in the value of M from a negative to a positive value as shown in Figure 5.

In the macroscopic forced string system, chaotic motion is numerically predicted[26] and experimentally verified[33] as generated through period-doubling bifurcations. The Shilnikov mechanism[34] is conjectured as the mechanism for chaotic motion.[26,35] This period-doubling phenomenon is also identified in our bifurcation diagram (Figure 3a and its

DOI: 10.1021/nl902775m | *Nano Lett.* **2010,** *10,* 406-413

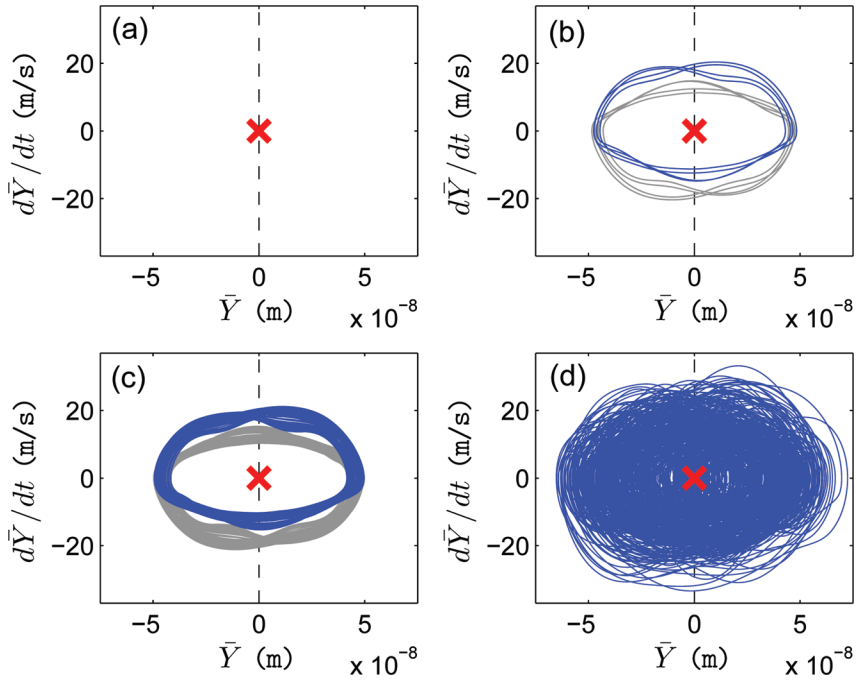

FIGURE 4. Phase-space representations of attractors for the nanowire system in distinct regimes: (a) planar-vibration (PV) state for V_{AC} = 0.594 V, (b) nonplanar vibration (NPV) state for V_{AC} = 6.88 V, (c) nonplanar chaotic vibration (NCV) state for V_{AC} = 6.9 V, and (d) nonplanar extensive chaotic vibration (NECV) state for V_{AC} = 6.96 V.

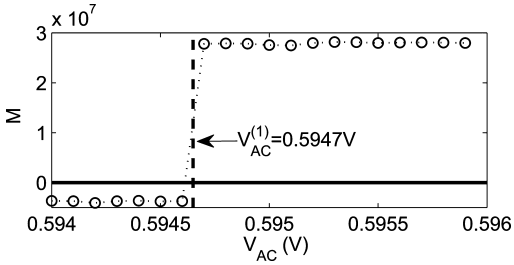

FIGURE 5. Escape exponent M as a function of V_{AC}. The PV−NPV transition occurs at $V_{AC}^{(1)} \approx 0.5947$ V.

inset) as the creation route of NCV state. In the classical theory of a forced damped string system, chaotic vibration is found to be generated from a branch of NPV which is separated (either isolated or connected by saddle-node bifurcations) from the NPV coming from PV through Hopf bifurcation.[26] In the electrostatically driven nanowire system, by examining the frequency response curve, we observed the same phenomenon that two branches are separated. In the theory of chaotic dynamical systems, the mechanism through which an extensive chaotic attractor with full-system symmetry is created is merging crisis,[36] where two coexisting chaotic attractors collide simultaneously with the boundary between their respective basins to merge into a larger attractor. The basin boundary is the stable manifold of a mediating unstable periodic orbit created at the original saddle−node bifurcation, where the node leads to the observed chaotic attractors through period-doubling bifurcations. If the system possesses certain symmetry, the merging crisis can restore the symmetry in the final, extensive chaotic attractor.[37] At the crisis, the gaps at all scales in and between the symmetry-broken attractors are filled,[38] due to the creation of new unstable periodic orbits through the horseshoe mechanism as a result of the "collision" of the chaotic attractors with the stable manifold of the mediating unstable periodic orbit (effectively homoclinic tangencies). All these have been established for dynamical systems of relatively low dimensions described by discrete-time maps or ordinary differential equations. O'Reilly et al.[39] analyzed a similar mechanism in macroscopic forced string system using a constructed Shilnikov type map and had identified the "homoclinic explosion" at which two symmetrical Rössler-like attractors disappeared and one Lorenz-like attractor was born. The numerical result of such phenomenon was also reported.[26] The phenomena described in these papers are similar to the generation process of the NECV state in electrostatic nanowire system. Note that, as compared with the macroscopic forced string systems, the complexity of equation is enhanced by nonlinear electrostatic force and by the square term of ac voltage which induces another frequency component of the excitation. Although the bifurcation mechanism could be similar, the resulted attractors may be qualitatively different, e.g., NECV versus NCV.

To explore the possibility of NECV in fabricated nanowire devices, we have simulated the PDE model (1) of an experimental device[21] operated under room conditions. The nanowire device has the dimensions of 4.9 μm × 88 nm ($L \times d$), which is suspended on the driving electrode with a gap of 250 nm. Setting excitation to be at resonant frequency f_0 =

DOI: 10.1021/nl902775m | *Nano Lett.* **2010,** *10,* 406-413

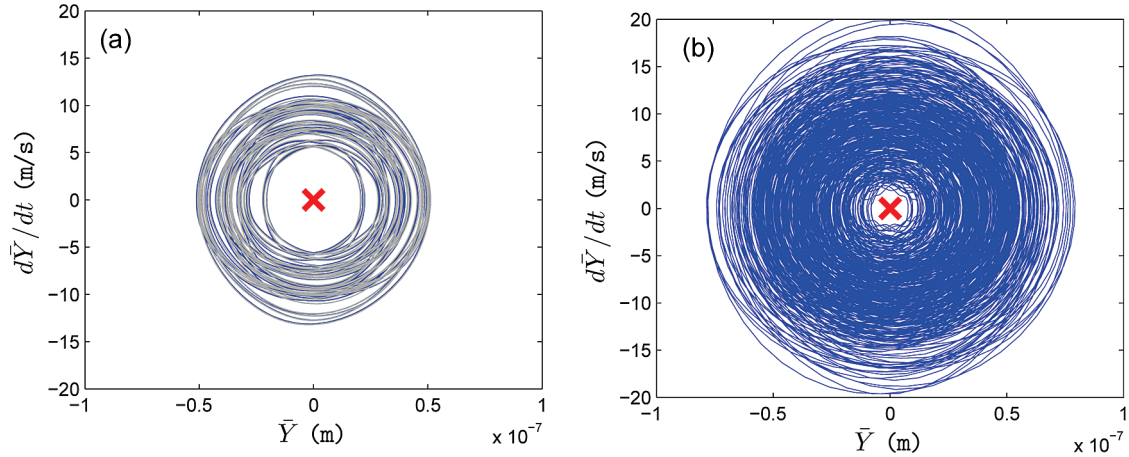

FIGURE 6. Phase-space representations of attractors for the nanowire system reported in experimental study.[21] (a) Nonplanar chaotic vibration (NCV) state for $V_{AC} = 20.0$ V and (b) nonplanar extensive chaotic vibration (NECV) state for $V_{AC} = 21.85$ V. The cross represents the planar vibration state (PV).

27.78 MHz and biasing the nanowire with $V_{DC} = 18.75$ V, we observe NCV and NECV, as shown in parts a and b of Figure 6, respectively. The NECV parameter region of ac voltage extends a few volts, indicating the feasibility of experimental observation.

We now articulate a potential application of extensive chaos. An important application of chaotic systems is random number generators (RNGs), which are commonly used in secure communication. RNGs based on chaotic oscillations have been realized in chaotic CMOS ICs[40] and quite recently in chaotic semiconductor lasers.[41] In such an application, the chaotic output is sensed by a transducer as an electrical signal and then transformed by an analog-to-digital converter (ADC) to a string of digital random numbers. The generating speed, system complexity, cost, reliability, and sensitivity to control parameters are among the considerations associated with RNGs. Due to potential advantages such as ultrahigh resonant frequency (e.g., gigahertz), relatively low fabrication cost, and small dimension, a chaotic nanowire-based resonator can be a promising candidate for minimization of highly integrated, high-speed RNGs.

In electrostatically driven MEMS and NEMS, previously reported nonextensive chaotic states (e.g., those generated though period-doubling bifurcations)[17] may not be useful for RNG applications, for the following two reasons. First, the degree of randomness associated with nonextensive chaotic motion may not be high enough for communication applications. Usually, nonextensive chaotic vibrations possess a strong periodic component.[17] In this case, the sampling rate must be low relative to the frequency of the underlying periodic component to overcome the strong autocorrelation in the displacement signal. Second, nonextensive chaotic states typically have fewer symmetries than those in the system itself. This lack of symmetry can produce bias in the generated random numbers. In order to overcome the bias, additional circuit components may be needed. The extensive chaotic state in electrostatically driven nanowires uncovered

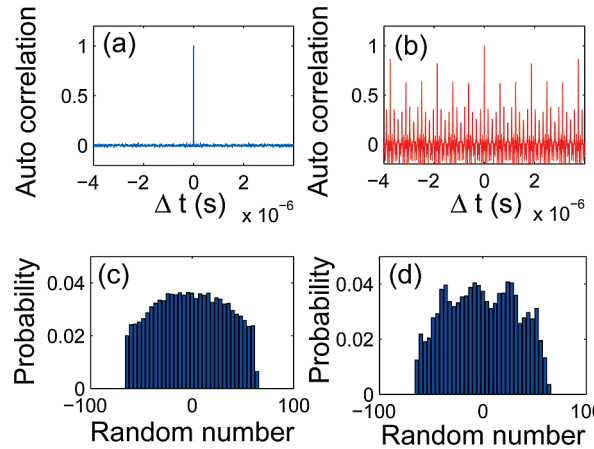

FIGURE 7. Autocorrelations of 7-bit random number sequences from (a) NECV and (b) NCV signals. (c, d) Distributions of 7-bit random numbers from the NECV and NCV signals, respectively.

in this Letter, however, naturally overcomes these two drawbacks. In particular, extensive chaos possesses a much higher degree of randomness than a nonextensive chaotic state. In addition, as we have demonstrated, the dynamical mechanism that generates an extensive chaotic state is symmetry-restoring.

To provide a concrete illustration of the advantage of exploiting extensive chaos in RNG applications, we compute and compare the RNG characteristics between NCV and NECV states in a Si nanowire of dimension 1 μm × 40 nm ($L \times d$), as shown in Figure 7. The sampling rate is set as the resonant frequency. The nanowire displacement signal in the Y direction is converted to an 8-bit digital number (including sign) in each sampling period and is then trimmed as a 7-bit digital number by removing the highest bit. Our results show that, although both NCV and NECV states are chaotic, the performances of using these two kinds of motion as RNG can be quite different. In particular, Figure 7a and Figure 7b illustrate the autocorrelations of the 7-bit random-

DOI: 10.1021/nl902775m | *Nano Lett.* **2010,** *10,* 406-413

number sequences from NCV and NECV, respectively. It can be seen that the autocorrelation associated with NECV is approximately a δ-function, signifying a much higher degree of randomness. Figure 7c and Figure 7d show the histograms of the sampled data from the NCV and NECV outputs, respectively. Apparently, the random numbers from the NECV signal are more evenly distributed than those from the NCV signal.

Further applications of extensive chaos in nanowires are the following.

(i) *Control of extensive chaos for desirable system performance*. NECV offers the ability to control the motion of the wire into any desirable state. In particular, a chaotic attractor has embedded within itself an infinite number of unstable periodic orbits and one can apply small perturbations to stabilize the motion of the wire about a desirable periodic orbit.[20] Since the nanowire is a driven dynamical system, we conceive using resonant perturbations to control chaos.[42] For example, in addition to the primary driving, a small driving signal of incommensurate frequency can be applied to stabilize the wire about an unstable periodic orbit. For extensive chaos, such an orbit can extend the dynamics into phase-space regions that were not accessible to the wire when it is in a PV, NPV, or even NCV state. Extensive chaos can also enrich, often significantly, the frequency response of the wire.

(ii) *Experimental setting of desirable initial state*. In the experiment to explore the basin structure of a bistable NEM device, it is necessary to spread the initial states of the system over the phase space.[5] This is usually done by using the method of stochastic interrogation,[43] where different initial conditions are realized by switching between stochastic and deterministic excitations. The existence of extensive chaos can facilitate this task, as the system can be driven into a NECV state first and then quickly switched back to the intended operational regime, where the initial condition is essentially the state of the system in the NECV regime before the switching.

In the above context, we consider the perfect model with ideal circular cross-section area. The imperfection, e.g., the residual stress (tensile or compressive) and initial slack with bow shape, could affect the creation of nonplanar motion.[9] Here, we shall describe and discuss how the prestress, initial slack, and imperfect cross-section area affect the generation of extensive chaotic motions. Tensile or compressive stress can be implemented in model (1) by modifying the stretching elastic nonlinear terms in the Z and Y directions as $-Z_{xx}[SA + EA/(2L)2L\int_0^L(Y_x^2 + Z_x^2)\,dx]$ and $-Y_{xx}[SA + EA/(2L)\int_0^L(Y_x^2 + Z_x^2)\,dx]$ where S is the residual tensile or compressive stress. The tensile force can harden the beam and enhance the linear resonant frequency. This effect shifts the onset of nonplanar motion[9] and is likely to increase the required excitation to generate NECV. To verify this conjecture, we simulate the nanowire with a tensile stress of $S =$ 7.4 MPa. The parameters of the wire are the same as those in in Figure 3 for which the stress can almost double the resonant frequency. In our simulations, we observe that the onset of V_{AC} for NECV increases by a few tens percent. On the other hand, compressive prestress can make the wire buckle. Our numerical observation shows that, with electrostatic excitation, the buckle of the beam will be led to the direction of electrostatic force. This is due to the fact that for a fully symmetrical rod, without external load, the buckle can happen to any arbitrary direction, but with the load, it is likely to be compliant to the external load's direction. The nanowire with compressive stress of $S = -7.4$ MPa is simulated. This value of stress causes 34 nm in the displacement of initial buckle at the center of the wire. In this case, it is observed that NECV exists and the onset of V_{AC} reduces by tens of percent from its stress-free value. This may be due to the initial prestress that makes the wire more unstable and more easily to undergo complex nonplanar rotation. Nanowire may have initial slack even without prestress due to imperfections in fabrication. In this case, model (1) needs to be modified as a curved beam model.[44] This effect will cause a symmetry breaking in the dynamical model and induce quadratic nonlinearity. Moreover, the slack can induce two eigenmodes with fixed directions and frequency mistuning.[9] To mimic the effect of initial slack, we add a constant force in the Y direction, which breaks the symmetry by biasing the beam for 37 nm in the Y axis. We also artificially double the resonant frequency in Y axis motion to mimic frequency mistuning. Simulation results show that NECV still exists but its onset has shifted by a few tens of percent. In reality, the nanowire may not have a perfectly circular cross-section shape. The imperfection can cause dual eigenmodes and frequency mismatch between the modes. The eigenmodes may not have a direction in the plane of excitation. These effects are similar to the case of a nanowire with initial slack and its effect to NECV is expected to be similar. In short, based on our simulation results, qualitatively speaking, the existence of NECV is robust for the effects of residual stress and fabrication imperfections.

In summary, we have carried out numerical simulations and analysis of a nonlinear PDE model for an electostatically driven Si nanowire, taking into account physical effects such as electrostatic and gas damping forces. A computationally intense bifurcation analysis reveals that the wire can be driven into chaos with symmetry breaking and then to extensive chaos by inheriting back the full symmetry of the system. Such an extensive chaotic state has not been predicted for nanoscale systems before, and we have articulated a number of potential applications including nanowire-based RNG. Exploiting nonlinear dynamics and chaos for nanodevices promises to be a potentially relevant area of research,[9] and we expect our findings to stimulate further work.

Acknowledgment. This work was supported by AFOSR under grant no. F9550-09-1-0260. This work was also sup-

DOI: 10.1021/nl902775m | *Nano Lett.* **2010,** *10,* 406-413

ported by the BBSRC under grants no. BB-F00513X and no. BB-G010722 and by the Scottish Northern Research Partnership. The authors thank Dr. Yan Wang and Dr. Wen-Xu Wang for many helpful discussions.

REFERENCES AND NOTES

(1) Yang, Y. T.; Callegari, C.; Feng, X. L.; Ekinci, K. L.; Roukes, M. L. *Nano Lett.* **2006**, *6*, 583.
(2) Rugar, D.; Budakian, R.; Mamin, H.; Chui, B. *Nature* **2004**, *430*, 329.
(3) Nguyen, C.-C. *IEEE Trans. Microwave Theory Tech.* **1999**, *47*, 1486.
(4) Kozinsky, I.; Postma, H. W. C.; Bargatin, I.; Roukes, M. L. *Appl. Phys. Lett.* **2006**, *88*, 253101.
(5) Kozinsky, I. ; Postma, H. W. Ch. ; Kogan, O.; Husain, A.; Roukes, M. L. *Phys. Rev. Lett.* **2007**, *99*, 207201.
(6) Cha, S. N.; Jang, J. E.; Choi, Y.; Amaratunga, G. A. J.; Kang, D. J.; Hasko, D. G.; Jung, J. E.; Kim, J. M. *Appl. Phys. Lett.* **2005**, *86*, 083105.
(7) Dequesnes, M.; Rotkin, S. V.; Aluru, N. R. *Nanotechnology* **2002**, *13*, 120.
(8) Postma, H. W. Ch.; Kozinsky, I.; Husain, A.; Roukes, M. L. *Appl. Phys. Lett.* **2005**, *86*, 223105.
(9) Conley, W.; Raman, A.; Krousgrill, C.; Mohammadi, S. *Nano Lett.* **2008**, *8*, 1590.
(10) Rueckes, T.; Kim, K.; Joselevich, E.; Tseng, G. Y.; Cheung, C.-L.; Lieber, C. M. *Science* **2000**, *289*, 94.
(11) Kim, P.; Lieber, C. M. *Science* **1999**, *286*, 2148.
(12) Aldridge, J. S.; Cleland, A. N. *Phys. Rev. Lett.* **2005**, *94*, 156403.
(13) Buks, E.; Yurke, B. *Phys. Rev. E* **2006**, *74*, 046619.
(14) Hu, S.; Raman, A. *Phys. Rev. Lett.* **2006**, *96*, 036107.
(15) Wang, Y. C.; Adams, S. G.; Thorp, J. S.; MacDonald, N. C.; Hartwell, P.; Bertsch, F. *IEEE Trans. Circuits Syst., I* **1998**, *45*, 1013.
(16) DeMartini, B. E.; Butterfield, H. E.; Moehlis, J.; Turner, K. L. *J. Microelectromech. Syst.* **2007**, *16*, 1314.
(17) De, S. K.; Aluru, N. R. *Phys. Rev. Lett.* **2005**, *94*, 204101. De, S. K.; Aluru, N. R. *J. Microelectromech. Syst.* **2006**, *15*, 355.
(18) Liu, S.; Davidson, A.; Lin, Q. *J. Micromech. Microeng.* **2004**, *14*, 1064.
(19) Karabalin, R. B.; Cross, M. C.; Roukes, M. L. *Phys. Rev. B.* **2009**, *79*, 165309.
(20) Ott, E.; Grebogi, C.; Yorke, J. A. *Phys. Rev. Lett.* **1990**, *64*, 1196. Pecora, L. M.; Carroll, T. L. *Phys. Rev. Lett.* **1990**, *64*, 821.
(21) He, R.; Feng, X. L.; Roukes, M. L.; Yang, P. *Nano Lett.* **2008**, *8*, 1756.
(22) Fung, W. Y.; Dattoli, E. N.; Lu, W. *Appl. Phys. Lett.* **2009**, *94*, 203104.
(23) Ekinci, K. L.; Roukes, M. L. R. *Rev. Sci. Instrum.* **2005**, *76*, 061101.
(24) Craighead, H. G. *Science* **2000**, *290*, 1532.
(25) Forsen, E.; Abadal, G.; Ghatnekar-Milsson, S.; Teva, J.; Verd, J.; Sandberg, R.; Svendsen, W.; Perez-Murano, F.; Esteve, J.; Campabadal, F.; Monelius, L.; Barniol, N.; Boisen, A. *Appl. Phys. Lett.* **2005**, *87*, 043507.
(26) Bajaj, A. K. ; Johnson, J. M. Philos. *Phys Trans. R. Soc. London* **1992**, *338*, 1.
(27) Grebogi, C.; Ott, E.; Yorke, J. A. *Phys. Rev. Lett.* **1982**, *48*, 1507.
(28) Gaillard, J.; Skove, M. J.; Ciocan, R.; Rao, A. M. *Rev. Sci. Instrum.* **2006**, *77*, 073907.
(29) Cimalla, V.; Foerster, Ch.; Will, F.; Tonisch, K.; Brueckner, K.; Stephan, R.; Hein, M. E.; Ambacher, O. *Appl. Phys. Lett.* **2006**, *88*, 253501.
(30) Yum, K.; Wang, Z.; Suryavanshi, A. P.; Yu, M.-F. *J. Appl. Phys.* **2004**, *96*, 3933.
(31) Desai, C. S.; Kundu, T. *Introductory finite element method*; CRC Press: Boca Raton, FL, 2001.
(32) Younis, M. I.; Alsaleem, F.; Jordy, D. *J. Non-linear Mech.* **2007**, *42*, 643.
(33) Molteno, T. C. ; Tufillar, N. B. *Am. J. Phys.* **2004**, *72*, 1157.
(34) Guckenheimer, J.; Holmes, P. *Nonlinear Oscillations, Dynamical Systems, and Bifurcations of Vector Fields*; Springer: New York. 1990.
(35) O'Reilly, O. M.; Holmes, P. J. *J. Sound Vib.* **1992**, *153* (3), 5365.
(36) Grebogi, C.; Ott, E.; Romeiras, F.; Yorke, J. A. *Phys. Rev. A* **1987**, *36*, 5365.
(37) Chossat, P.; Golubitsky, M. *Physica D* **1988**, *32*, 423.
(38) Szabó, K.; Lai, Y.-C.; Tél, T.; Grebogi, C. *Phys. Rev. Lett.* **1996**, *77*, 3102. Szabó, K.; Lai, Y.-C.; Tél, T.; Grebogi, C. *Phys. Rev. E* **2000**, *61*, 5019.
(39) O'Reilly, O. M. *Int. J. Non-linear Mech.* **1993**, *28*, 337.
(40) Drutarovsky, M.; Galajda, P. *J. Electr. Eng.* **2006**, *57*, 218.
(41) Reidler, I.; Aviad, Y.; Rosenbluh, M.; Kanter, I. *Phys. Rev. Lett.* **2009**, *103*, 024102.
(42) Braiman, Y.; Goldhirsch, I. *Phys. Rev. Lett.* **1991**, *66*, 2545. Chacón, R. *Phys. Rev. Lett.* **2001**, *86*, 1737.
(43) Cusumano, J. P.; Kimble, B. W. *Nonlinear Dyn.* **1995**, *8*, 213.
(44) Nayfeh, A. H.; Balachandran, B. *Appl. Mech. Rev.* **1989**, *42*, 175.

DOI: 10.1021/nl902775m | *Nano Lett.* **2010,** *10,* 406-413